

Scaling phenomena driven by inhomogeneous conditions at first-order quantum transitions

Massimo Campostrini¹, Jacopo Nespolo¹, Andrea Pelissetto², and Ettore Vicari¹

¹ *Dipartimento di Fisica dell'Università di Pisa and INFN, Largo Pontecorvo 3, I-56127 Pisa, Italy and*

² *Dipartimento di Fisica dell'Università di Roma "La Sapienza" and INFN, Sezione di Roma I, I-00185 Roma, Italy*

(Dated: November 11, 2014)

We investigate the effects of smooth inhomogeneities at first-order quantum transitions (FOQT), such as those arising from the presence of a space-dependent external field, which smooths out the typical discontinuities of the low-energy properties. We argue that scaling phenomena develop at the transition region where the external field takes the value corresponding to the FOQT of the homogenous system. We present numerical evidence of such scaling phenomena at the FOQTs of quantum Ising chains, driven by a parallel magnetic field when the system is in the ferromagnetic phase, and at the FOQT of the q -state Potts chain for $q > 4$, driven by an even temperature-like parameter giving rise to a discontinuity of the ground-state energy density.

PACS numbers: 05.30.Rt, 64.60.fd, 64.60.De

I. INTRODUCTION

The theories of *classical* and *quantum* phase transitions^{1–3} generally apply to homogenous systems. However, homogeneity is often an ideal limit of experimental conditions. Inhomogeneous conditions generally smooth out the singularities at phase transitions. This is also expected at first-order transitions which are characterized by discontinuities in the thermodynamic quantities at classical finite-temperature transitions, or in the properties of the ground state at first-order quantum transitions (FOQTs).

In the presence of smooth inhomogeneities, we may simultaneously observe different phases at different space regions, separated by crossover regions where the system passes from one phase to the other one, developing critical correlations. For example, this scenario is observed in typical cold-atom experiments⁴, where the atoms are constrained in a limited space region by an inhomogeneous (usually harmonic) trap, which effectively makes the chemical potential space dependent.

The effects of the inhomogeneous conditions have been much investigated at continuous transitions^{4–46}. For sufficiently smooth inhomogeneities, classical or quantum systems, at classical (finite-temperature) or quantum (zero-temperature) transitions, develop scaling phenomena with respect to the length scale ℓ induced by the inhomogeneity. These scaling behaviors are controlled by the universality class of the transition of the homogenous system. They have some analogies with the standard finite-size scaling (FSS) theory for homogenous systems^{47,48}, with two main differences: the inhomogeneity due to the space-dependence of the external field characterized by the length scale ℓ , and a nontrivial power-law dependence of the correlation length ξ when increasing ℓ at the critical point, i.e. $\xi \sim \ell^\theta$, where θ is a universal exponent depending on some general features of the external space-dependent field.^{19,25}

Scaling phenomena also emerge at first-order classical transitions in the presence of a temperature gradient⁴⁶ or

a space-dependent external field. They are observed in the transition region where the space-dependent temperature assumes values close to the critical temperature of the homogenous system. The discontinuities of the homogenous system in the thermodynamic limit turn out to be reconstructed through scaling behaviors characterized by nontrivial power laws, whose main features turn out to be quite similar to those at continuous transitions.

In this paper we study the effects of inhomogeneous conditions at FOQTs. FOQTs are also of great interest, as they occur in a large number of quantum many-body systems, such as quantum Hall samples⁴⁹, itinerant ferromagnets⁵⁰, heavy fermion metals^{51–53}, etc. They are also expected in multicomponent cold-atom systems in optical lattices, with spin-orbit coupling and synthetic gauge fields, which lead to various phases with some quantum transitions of first order, see, e.g., Refs. 54–58.

We investigate the scaling phenomena arising when one of the model parameters smoothly depends on the space, smoothing out the discontinuities of the ground state. We put forward a scaling theory which describes the low-energy properties in the crossover space region where the system changes phase. We apply this scaling theory to relatively simple quantum many-body systems, such as quantum Ising and Potts chains driven across their FOQTs by space-dependent magnetic fields, and check its predictions against numerical results.

The paper is organized as follows. In Sec. II we present the quantum Ising and Potts chains with external space-dependent magnetic fields; we also show some numerical results for their behavior around the spatial point corresponding to the parameter values of the FOQT. In Sec. III we put forward scaling ansatzes to describe the scaling phenomena in the crossover region around the transition point. In Sec. IV we check these scaling theory by analyzing the numerical results of the Ising and Potts chains. Finally, in Sec. V we draw our conclusions.

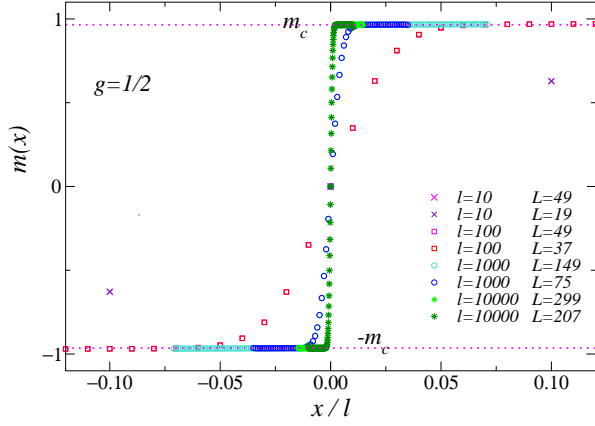


FIG. 1: (Color online) The local magnetization $m(x) \equiv \langle \sigma_x^{(1)} \rangle$ for the Ising chain (1) with $g = 1/2$ and $h_x = x/\ell$, versus x/ℓ . The dotted lines indicate the transition values $m_{\pm} = \pm m_c$, cf. Eq. (8). The data for the same ℓ and different L turn out to be indistinguishable, showing that they effectively provide the $L \rightarrow \infty$ limit.

II. QUANTUM ISING AND POTTS CHAINS

In order to make our scaling arguments more concrete, we first present the quantum models that we use as theoretical laboratories for scaling phenomena at FOQTs in the presence of a spatial inhomogeneity. We consider the FOQTs of the Ising chains in the ordered phase driven by a *parallel* magnetic field coupled to the order-parameter spin operators, and the FOQTs of quantum q -state ($q > 4$) Potts chains driven by a *transverse* magnetic field.

We also present numerical results obtained using standard implementations of the density matrix renormalization-group (DMRG) method⁵⁹. Some details of the DMRG implementations can be found in Refs. 60,61 where we presented numerical analyses of the same models in homogenous conditions. The inhomogeneous conditions that we consider here do not lead to further particular problems from the numerical point of view.

A. The quantum Ising chain

We consider a quantum Ising chain of size $2L + 1$ with a space-dependent parallel magnetic h_x along the order-parameter spin operator, i.e.

$$H_I = -J \sum_{x=-L}^{L-1} \sigma_x^{(1)} \sigma_{x+1}^{(1)} - g \sum_{x=-L}^L \sigma_x^{(3)} - \sum_{x=-L}^L h_x \sigma_x^{(1)}, \quad (1)$$

where $\sigma_x^{(a)}$ are the Pauli matrices, $g \geq 0$ is a transverse magnetic field, and h_x is a space-dependent magnetic

field

$$h_x \equiv h(x/\ell), \quad (2)$$

where ℓ is a length scale. The most interesting case is a linear space dependence

$$h(x) = x. \quad (3)$$

Indeed, it may be also considered as a local effective linear approximation of a more general dependence, i.e.

$$h(x) \approx a_1(x - x_0) + a_2(x - x_0)^2 + \dots \quad (4)$$

around the point x_0 where it vanishes, corresponding to the FOQT value. It is also convenient to extend the analysis to a more general power law of the space dependence

$$h(x) = \text{sgn}(x) |x|^p, \quad (5)$$

to crosscheck the scaling theory we shall put forward to describe these phenomena. We study the system in the $L \rightarrow \infty$ limit and investigate the scaling behavior with respect to the remaining length scale ℓ . In the following we set $J = 1$.

Note that the $p \rightarrow \infty$ limit of Eq. (5) corresponds to a homogenous system with $L = \ell$ and fixed opposite (kink-like) boundary conditions (FOBC), which may be described by the standard Ising-chain Hamiltonian with a boundary term⁶⁰

$$H_{I,\text{FOBC}} = - \sum_{x=-L}^{L-1} \sigma_x^{(1)} \sigma_{x+1}^{(1)} - g \sum_{x=-L}^L \sigma_x^{(3)} - (\sigma_{-L}^{(1)} - \sigma_L^{(1)}). \quad (6)$$

The last term between parenthesis is added to achieve FOBC, indeed it arises when adding further fictitious sites at $-L - 1$ and $L + 1$ which are eigenstates of $\sigma^{(1)}$ with opposite ± 1 eigenvalues respectively.

The homogenous Ising chain, i.e. the model (1) with constant magnetic field $h_x = h$, has a continuous transition at $g = 1$, $h = 0$, belonging to the two-dimensional Ising universality class. This quantum critical point separates a paramagnetic ($g > 1$) and a ferromagnetic ($g < 1$) phase. In the ferromagnetic phase $g < 1$, the parallel magnetic field h drives a FOQT at $h = 0$, with a discontinuity of the magnetization, i.e. the ground-state expectation value of $\sigma_x^{(1)}$. Indeed, neglecting boundary effects, we have⁶²

$$m_{\pm} = \lim_{h \rightarrow 0^{\pm}} \lim_{L \rightarrow \infty} \langle \sigma_x^{(1)} \rangle = \pm m_c, \quad (7)$$

$$m_c = (1 - g^2)^{1/8}. \quad (8)$$

Therefore, in the presence of an inhomogeneous field which vanishes at $x = 0$ changing sign, such as that in Eq. (3), the point $x = 0$ effectively corresponds to a spatial transition point where the system experiences a

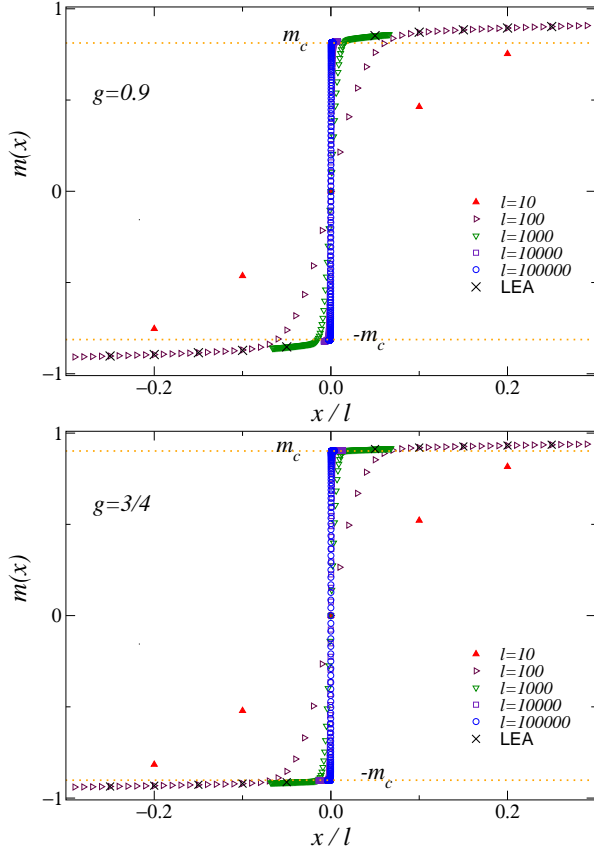


FIG. 2: (Color online) The local magnetization $m(x)$ of the model (1) with $h_x = x/\ell$, for $g = 3/4$ (bottom) and $g = 9/10$ (top). The values of m_c are given by Eq. (8). We also show data computed using the LEA, obtained by DMRG computations of the homogenous systems.

transition between two magnetized phases with opposite sign, i.e. with $\langle \uparrow | \sigma_x^{(1)} | \uparrow \rangle = m_+$ and $\langle \downarrow | \sigma_x^{(1)} | \downarrow \rangle = m_-$.

Some numerical DMRG results for the space dependence of the local magnetization

$$m(x) = \langle \sigma_x^{(1)} \rangle \quad (9)$$

are shown in Figs. 1, 2 and 3 for linearly and quadratically varying fields $h(x)$. They are obtained for sufficiently large size L , to effectively provide their $L \rightarrow \infty$ limit at fixed ℓ around the region where $h(x)$ vanishes. This is easily checked by comparing data with the same ℓ and increasing L ; some examples are reported in Figs. 1 and 3. Note that, with increasing ℓ , we need smaller and smaller ratios L/ℓ to achieve the large L limit for the energy differences of the lowest levels, and the observables around $x = 0$. This will be explained by the scaling theory of Sec. III, which shows that the relevant scaling length in the crossover region around $x = 0$ is $\xi \sim \ell^\theta$ with $\theta = 1/4$ for linear $h(x)$, and $\theta = 2/5$ for the quadratic dependence. Therefore, the relevant ratio for the crossover region is L/ℓ^θ , instead of L/ℓ .

The data around $x = 0$ show a crossover between the two magnetization values m_\pm , cf. Eq. (7), which becomes

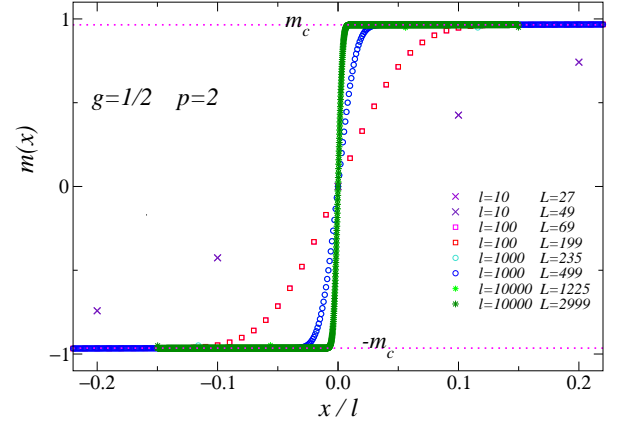


FIG. 3: (Color online) The local magnetization $m(x)$ for the Hamiltonian (1) with quadratic space dependence ($p = 2$) of h_x at $g = 1/2$. The data for the same ℓ and different L practically coincide, showing that they are already a good approximation of the $L \rightarrow \infty$ limit.

sharper and sharper with increasing ℓ . The comparison between linear and quadratic dependences of h_x , see in particular Figs. 1 and 3 for the same value $g = 1/2$, show similar behaviors, only the crossover region appears enlarged.

In noncritical regimes, away from phase transitions when correlations do not develop long length scales, inhomogeneity effects can be effectively taken into account by local-equilibrium approximations (LEA), assuming a local equilibrium analogous to that of the homogenous system at the same fixed parameters. An example is the local-density approximation widely used to study particle systems with an effective space-dependent chemical potential, see, e.g., Refs 4,32,63–66. However, when correlations develop large length scales, such as at classical and quantum transitions, LEA may not provide a satisfactory description, and significant corrections are found^{32,39,66}. This failing of the LEA is also observed at first-order classical transition in the presence of a temperature gradient⁴⁶.

We compare the results for the inhomogeneous Ising model with the LEA $m_{\text{lea}}(x)$, which estimates $m(x)$ using the corresponding values $m_h(h)$ of the homogenous system in the infinite volume limit at the given value of h_x , i.e.

$$m(x) \approx m_{\text{lea}}(x/\ell) = m_h[h(x/\ell)] \quad (10)$$

Note that since the external field h_x is a function of the ratio x/ℓ , the LEA scales as x/ℓ . LEA is expected to provide a good approximation when h_x varies smoothly, thus for large ℓ . However, since the magnetization value of the homogenous system lies within $1 \geq |m| \geq m_c$, LEA can not describe the crossover region where $|m| < m_c$.

Some LEA results are shown in Fig. 2. The data at fixed x/ℓ appear to approach their LEA with increasing ℓ . This convergence is fast far from $x = 0$, but it becomes significantly slower when approaching $x = 0$, i.e. it is

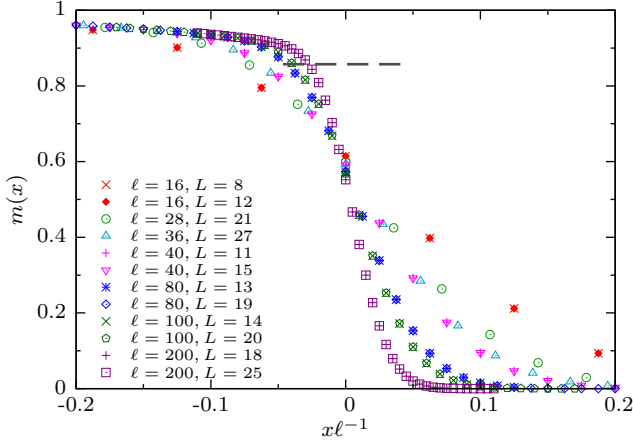


FIG. 4: The local magnetization $m(x)$ of the quantum $q = 10$ Potts chain in the presence of a linear transverse field. The dashed line indicates the value $m_c = 0.8572$ defined in Eq. (20). The data for the same ℓ and different L practically coincide, showing that they are already asymptotic and do not depend on L .

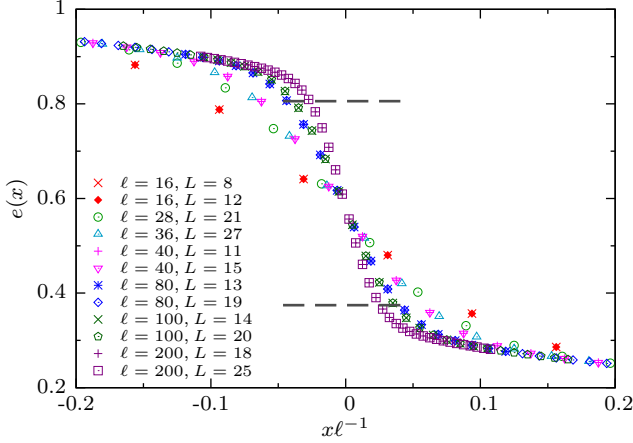


FIG. 5: The energy density $e(x)$, cf. Eq. (16), of the quantum $q = 10$ Potts chain in the presence of a linear transverse field. The dashed lines indicate $e_- = 0.8060$ and $e_+ = 0.3745$ defined in Eq. (17). The data for the same ℓ and different L practically coincide, showing that they are already asymptotic and do not depend on L .

non uniform when $|x| \rightarrow 0$. As we shall see, this reflects a hidden nontrivial scaling behavior which characterizes the crossover region around $x = 0$ in the smooth $\ell \rightarrow \infty$ limit, and requires nontrivial power-law rescalings of the distances from $x = 0$. This is a novel regime, somehow probing the mixed quantum phase where $-m_c < m(x) < m_c$.

B. The quantum Potts chain

Examples of FOQTs driven by even temperature-like parameters are provided by the quantum q -state Potts

chains for $q > 4$, which are the quantum counterpart of the classical two-dimensional Potts models^{67–69}

$$H_c = -J \sum_{\langle ij \rangle} \delta(s_i, s_j), \quad (11)$$

where the sum is over the nearest-neighbor sites of a square lattice, s_i are spin variables taking q integer values, i.e. $s_i = 1, \dots, q$, and $\delta(m, n) = 1$ if $m = n$ and zero otherwise. The quantum Hamiltonian can be derived from the *time* continuum limit of the transfer matrix, with q states per site, which can be labeled by an integer number $|n = 1\rangle, \dots, |n = q\rangle$. For a chain of size $2L + 1$ it reads^{61,70,71}

$$H_P = - \sum_{x=-L}^{L-1} \sum_{k=1}^{q-1} \Omega_x^k \Omega_{x+1}^{q-k} - g \sum_{x=-L}^L \sum_{k=1}^{q-1} M_x^k - \sum_{k=1}^{q-1} \Omega_{-L}^k \quad (12)$$

where Ω_x and M_x are $q \times q$ matrices:

$$\Omega = \delta_{m,n} \omega^{n-1}, \quad \omega = e^{i2\pi/q}, \quad (13)$$

$$M = \delta_{m, \text{Mod}(n-1, q)} = \begin{pmatrix} 0 & 1 & & \\ & \ddots & \ddots & \\ & & \ddots & 1 \\ 1 & & & 0 \end{pmatrix}. \quad (14)$$

These matrices commute on different sites and satisfy the algebra: $\Omega_x^k \Omega_x^l = \Omega_x^{k+l}$, $M_x^k M_x^l = M_x^{k+l}$, $\Omega_x^q = M_x^q = \mathbb{I}$, $M_x^k \Omega_x^l = \omega^{kl} \Omega_x^l M_x^k$.

Last term in the r.h.s. of Eq. (12) is a boundary term which softly breaks the q -state symmetry favoring the state $n = 1$. It ensures the self-dual property⁷¹

$$H_P(g) = g H_P(1/g) \quad (15)$$

even for finite chains⁶¹. The Hamiltonian H_P corresponds to a chain with mixed self-dual boundary conditions (SDBC), with a fixed state $n = 1$ at a further site $x = -L - 1$, and an unmagnetized disordered state $\propto \sum_{n=1}^q |n\rangle$ at $x = L + 1$.

In the case of $q = 2$ states the Hamiltonian H_P describes a quantum Ising chain with mixed fixed-free boundary conditions.

Like quantum Ising chains, the low-energy properties of the quantum Potts chains show two phases: a disordered phase for sufficiently large values of g and an ordered phase for small g where the system magnetizes along one of the q *directions*. The transition point is easily inferred from the duality relation (15), obtaining $g = g_c = 1$. For $q > 4$ the two phases are separated by a FOQT where the energy density and magnetization are discontinuous^{68–71}.

The FOQTs of the Potts chains are characterized by a discontinuity of the energy density of the ground state. We define the energy density as

$$e(x_b) = \langle \mathcal{E}_x \rangle, \quad \mathcal{E}_x = \delta(n_x, n_{x+1}) = \frac{1}{q} \sum_{k=1}^q \Omega_x^k \Omega_{x+1}^{q-k}, \quad (16)$$

where $x_b = x + 1/2$ is the position of the bond center. The infinite-volume energy density changes discontinuously across the FOQT, i.e. the two limits

$$e_{\pm} = \lim_{g \rightarrow 1^{\pm}} \lim_{L \rightarrow \infty} e(x) \quad (17)$$

differ at the FOQTs of the Potts chains with $q > 4$. Their difference $\Delta e \equiv e_+ - e_-$ is the analog of the latent heat of first-order finite-temperature transitions. For example,⁶¹ for the $q = 10$ Potts chain $e_- = 0.8060(1)$ and $e_+ = 0.3745(5)$.

Also the magnetization is discontinuous at the transition, passing from zero in the disorder ($g > 1$) phase to nonzero in the ordered ($g < 1$) phase. We define the local magnetization of the ground state as

$$m(L, g, x) = \langle \mathcal{M}_x \rangle, \quad (18)$$

$$\mathcal{M}_x = \frac{q\delta(n_x, 1) - 1}{q - 1}, \quad \delta(n_x, 1) = \frac{1}{q} \sum_{k=1}^q \Omega_x^k. \quad (19)$$

The limit

$$m_c = \lim_{g \rightarrow 1^-} \lim_{b \rightarrow 0} \lim_{L \rightarrow \infty} m(x) \quad (20)$$

is non zero for $q > 4$, where b is a *magnetic* field coupled to the global projector to the $n = 1$ state, e.g. described by the Hamiltonian term

$$H_{Pb} = -b \sum_{x=-L}^L \sum_{k=1}^q \Omega_x^k. \quad (21)$$

For example, numerical results for $q = 10$ give⁶¹ $m_c = 0.8572(1)$.

Again, we extend the homogenous model (12) to allow for a space-dependent *transverse magnetic* field. This is achieved by adding

$$H_{Ph} = - \sum_{x=-L}^L h_x \sum_{k=1}^{q-1} M_x^k \quad (22)$$

to the Hamiltonian (12), where h_x may have a linear space dependence such as Eq. (3), or a more general power law such as Eq. (5). We fix the parameter g of the Hamiltonian H_P to its critical value $g = g_c = 1$, so that at the center $x = 0$ of the chain the parameters take the values of the FOQT. Moreover, we consider $L \leq \ell$ so that the local transverse field satisfies $g + h_x > 0$. Again when we consider external fields (5) in the limit $p \rightarrow \infty$, we recover the homogenous system with SDBC.

In Fig. 4 we show DMRG results for the local magnetization $m(x)$ of the q -state Potts chain with $q = 10$ in the presence of a linearly space-dependent field h_x , cf. Eq. (3). They show that the local magnetization rapidly drops in the space region corresponding to the disordered phase, i.e. $x > 0$.

Data for the energy density, and its space dependence, are shown in Fig. 5. They clearly show a crossover region where the data pass from $e(x) \gtrsim e_-$ to $e(x) \lesssim e_+$, which

are the values of the energy density corresponding to the ordered and disordered phase respectively.

The data of the energy differences of the lowest states, and the observables around $x = 0$, i.e. for sufficiently small ratios x/ℓ , rapidly converge when increasing the ratio L/ℓ keeping ℓ fixed. Like the Ising case, this is checked by comparing data with increasing L , as shown in Figs. 4 and 5. For example, in the case of $\ell = 200$, $E_1 - E_0 = 0.90956$ for $L = 18$ and $E_1 - E_0 = 0.90952$ for $L = 25$. Analogous precision is achieved for the other observables around $x = 0$, and sufficiently far from the boundaries. Again, with increasing ℓ smaller and smaller ratios L/ℓ are sufficient to effectively obtain L -independent results. This is essentially related to the fact the relevant scaling length in the crossover region around $x = 0$ is $\xi \sim \ell^\theta$ with $\theta = 1/3$ for linear $h(x)$, as argued in Sec. III.

Note that, since the Potts chain with $q = 10$ is much more complex than the Ising chain, DMRG computations allow us to get reliable results for smaller chain sizes, and therefore smaller length scales of the external magnetic field. This is essentially related to the fact that many more states per site must be kept in the computations.

III. SCALING BEHAVIOR AT THE CROSSOVER SPACE REGION

In this section we present a scaling theory for the behaviors observed at the FOQTs of the Ising and Potts chains in the presence of inhomogeneous external fields.

For this purpose we first consider the $p \rightarrow \infty$ limit of the external field (5), which corresponds to homogenous systems of finite size with appropriate boundary conditions. In the case of the FOQTs of the Ising chains the resulting boundary conditions are FOBC, see Sec. II A and in particular Eq. (6). In the case of the FOQTs of the Potts chain, see Sec. II B, the $p \rightarrow \infty$ limit corresponds to the homogenous system with SDBC, i.e. Eq. (12) with $h_x = 0$.

Therefore, in the $p \rightarrow \infty$ limit the scaling behavior must match the finite-size behavior of homogeneous systems at FOQTs. Although FOQTs do not develop a diverging correlation length in the infinite-volume limit, they show FSS behaviors around the transition point, both in the case of classical and quantum first-order transitions^{60,61,71–83}. The FSS at FOQTs turns out to be particularly sensitive to the boundary conditions. Indeed, the size dependence of the scaling variables may significantly change when varying the boundary conditions.^{60,61} For example, in the case of the FOQTs of Ising chains, driven by a magnetic field in their ordered quantum phase, we have an exponential size dependence for open and periodic boundary conditions, while it is power law for antiperiodic or kink-like FOBC boundary conditions.⁶⁰ Actually, this particular sensitiveness to the boundary conditions is a peculiar feature of FOQTs, which qualitatively distinguish their FSS behaviors

from those at continuous quantum transitions, see e.g. Refs. 84,85.

The relevant *scaling* variable of FSS at FOQTs is given by the ratio $\kappa = E_L/\Delta_L$ between the energy contribution E_L of the perturbation driving the transition and the energy difference (*gap*) of the lowest states $\Delta_L \equiv E_1 - E_0$ at the transition point. The particular sensitiveness to the boundary conditions essentially arises from the gap Δ_L entering the scaling variable κ , whose finite-size behavior depends crucially on the boundary conditions considered. At the FOQTs ($h = 0$) of the Ising chain with FOBC the gap behaves as⁶⁰

$$\Delta_L \sim L^{-z}, \quad z = 2, \quad (23)$$

which may be associated with a dynamic exponent $z = 2$. In the case of FOQTs of the Potts chain with SDBC it behaves as⁶¹

$$\Delta_L \sim L^{-z}, \quad z = 1, \quad (24)$$

thus corresponding to a dynamic exponent $z = 1$.

At the FOQTs of the Ising chain driven by the parallel magnetic field h , the relevant scaling variable of its FSS with FOBC is⁶⁰

$$\kappa_I = hL/\Delta_L \sim hL^{d+z} = hL^3. \quad (25)$$

In the language of the renormalization-group (RG) theory, this relation allows us to associate a RG dimension with the perturbation h , given by

$$y_h = d + z = 3. \quad (26)$$

The FOQTs of the Potts chains for $q > 4$ is driven by the model parameter g . Setting the perturbation $h \equiv g - 1$ at the transition point $g = 1$, the relevant scaling variable for SDBC turns out to be⁶¹

$$\kappa_P = hL/\Delta_L \sim hL^{d+z} = hL^2. \quad (27)$$

Thus

$$y_h = d + z = 2 \quad (28)$$

is the RG dimension of $h = g - 1$ describing the FSS at the FOQTs of the Potts chains with SDBC.

The above considerations imply that the space dependence is controlled by the scaling variable

$$x/L \sim xh^{1/y_h} \quad (29)$$

to keep $\kappa_{I,P}$ fixed. We want to extend the FSS ansatzes⁶⁰ holding for the homogenous systems, thus in the limit $p \rightarrow \infty$, to allow for a power-law space dependence of the external fields. The scaling variables in the presence of inhomogenous fields characterized by the power law p , cf. Eq. (5), can be heuristically derived by replacing the perturbation parameter h with $h_x \sim (x/\ell)^p$ in Eq. (29). Therefore, assuming that the scaling behavior remains

controlled by the RG dimension y_h , and that the chain size L is sufficiently large not to play any role, we obtain

$$x \left(\frac{x}{\ell} \right)^{p/y_h} = \left(\frac{x}{\ell^\theta} \right)^{1+p/y_h}, \quad (30)$$

where the exponent θ is given by

$$\theta = \frac{p}{p + y_h}, \quad (31)$$

with y_h given by Eqs. (26) and (28) for the FOQTs of Ising and Potts chains respectively. The relation (30) suggests that the relevant scaling in the presence of inhomogeneous external fields is obtained by keeping the scaling variable

$$X = x/\ell^\theta \quad (32)$$

fixed. This implies that the observables and correlations in the crossover region around the transition point develop a length scale ξ , behaving as

$$\xi \sim \ell^\theta. \quad (33)$$

Note that $\theta \rightarrow 1$ for $p \rightarrow \infty$ consistently with the fact that we must recover the FSS of homogenous systems in this limit.

On the basis of these considerations we expect that the asymptotic large- ℓ behavior of the energy difference Δ_ℓ of the two lowest levels scales as

$$\Delta_\ell \sim \xi^{-z} \sim \ell^{-z\theta} \quad (34)$$

with θ given by Eq. (31), and z is the effective dynamic exponent read from the size dependence of the gap at the transition point.

Around the point where $h(x)$ vanishes, the local magnetization is expected to asymptotically behave as

$$m(x) = m_c f_m(X), \quad X = x/\ell^\theta, \quad (35)$$

where m_c , cf. Eqs. (7) and (20), is the normalization such that $\lim_{X \rightarrow -\infty} f_m(X) = -1$ in the Ising case, and $\lim_{X \rightarrow -\infty} f_m(X) = 1$ in the Potts case. We also consider the two-point function of the order parameter. In the case of the Ising chain it is defined as

$$G(x, y) = \langle \sigma_x^{(1)} \sigma_y^{(1)} \rangle. \quad (36)$$

In the case of the Potts chain we consider the two-point correlation function

$$G(x, y) = \langle \mathcal{M}_x \mathcal{M}_y \rangle, \quad (37)$$

and its connected part

$$G_c(x, y) = \langle \mathcal{M}_x \mathcal{M}_y \rangle - \langle \mathcal{M}_x \rangle \langle \mathcal{M}_y \rangle, \quad (38)$$

with \mathcal{M}_x defined in Eq. (19). Around the region where h vanishes, we expect the scaling behavior

$$G(x_1, x_2) \approx m_c^2 f_g(X_1, X_2). \quad (39)$$

An analogous scaling is expected for its connected part $G_c(x_1, x_2)$. The scaling functions f_m and f_g are expected to be universal, i.e. largely independent of the microscopic details of the model. For example, in the case of the FOQT of Ising chains, they are expected to be independent of the particular value of g within the quantum ordered phase, apart from a trivial (and unique) rescaling of their arguments.

When the FOQT gives rise to a discontinuity in the energy density, such as the FOQT of quantum Potts chains with $q > 4$ at $g = 1$, we expect that its asymptotic behavior around $x = 0$ is

$$e(x) \approx f_e(X). \quad (40)$$

Moreover, the scaling function f_e is expected to have the value e_{\pm} , cf. Eq. (17), as asymptotic limits, i.e.

$$\lim_{X \rightarrow \pm\infty} f_e(X) = e_{\pm}. \quad (41)$$

essentially because it describes the crossover between the two pure phases where the energy density of the system takes the values e_{\pm} .

The above large- ℓ scaling ansatzes are expected to be approached with $O(\ell^{-\theta})$ corrections. Note that they also imply that the curves for different values of ℓ cross each other around $x = 0$, as shown in Figs. 1-5, and this crossing point approaches the point X_c (where $X = x/\ell$) corresponding to $g = g_c$. Actually, one may exploit this property to estimate the critical parameter g_c when it is not known, using a linear spatial dependence of g (for which the point $x = 0$ is not particular) and looking at the crossing point of the energy density and magnetization data. The results are expected to approach X_c , thus g_c , with $O(\ell^{-1})$ corrections.

It is important to note that, in the case of more general space dependences such as that in Eq. (4), the linear term determines the scaling behavior at the crossover region, obtained keeping $X \equiv x/\ell^\theta$ fixed with $\theta = (1 + y_h)^{-1}$, cf. Eq. (31) with $p = 1$, while higher-order terms give rise to $O(\ell^{-1+\theta})$ corrections.

Although the above discussion focuses on the FOQTs of the Ising and Potts chains, the scaling ansatzes at FOQTs in the presence of inhomogeneous fields can be straightforwardly extended to general FOQTs, and higher dimensions.

Finally, we note that similar scaling behaviors have been conjectured, and numerically checked, at classical first-order transitions in the presence of a temperature gradient⁴⁶.

IV. SCALING PHENOMENA INDUCED BY THE INHOMOGENEOUS FIELDS

In this section we show that the numerical results for the Ising and Potts chains in the presence of inhomogeneous magnetic fields support the scaling behaviors put forward in Sec. III. We study the scaling behavior with

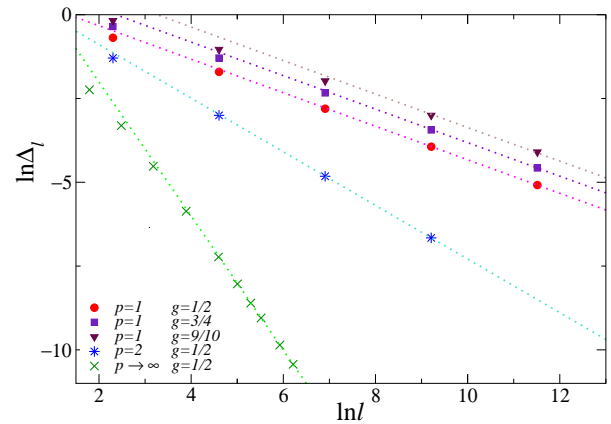


FIG. 6: (Color online) The gap Δ_ℓ as a function of ℓ for the Hamiltonian (1), for magnetic fields h_x with power laws $p = 1$, $p = 2$ and $p \rightarrow \infty$. The dotted lines show the expected behavior $\Delta \sim \ell^{-2\theta}$ with $\theta = 1/4$ for $p = 1$, $\theta = 2/5$ for $p = 2$, and $\theta = 1$ for $p = \infty$.

respect to the length scale ℓ only; as already discussed in Sec II, the data that we present are obtained for sufficiently large L , so that their behaviors in the crossover region do not effectively depend on L anymore.

A. Results for the Ising chain

Fig. 6 shows the dependence on the length scale ℓ of the energy difference Δ_ℓ of the lowest states for various values of p , i.e. $p = 1, 2$ and $p \rightarrow \infty$ corresponding to homogenous systems with FOBC. They confirm the predicted behavior $\Delta_\ell \sim \ell^{-2\theta}$, cf. Eq. (34) with $z = 2$.

In Fig. 7 we show results for the local magnetization $m(x)$ and the two-point function $G(0, x)$ in the case of a linear dependence ($p = 1$) of h_x , for which $\theta = 1/4$, at three values of g to check universality, i.e. $g = 1/2, 3/4, 9/10$. They nicely confirm the asymptotic scaling behavior predicted by the Eqs. (35) and (39), and the universality of the scaling functions f_m and f_g with respect to g , apart from a trivial rescaling of its argument.

Like the homogenous system with kink-like FOBC, we expect the lowest energy states are associated with domain walls (kinks), i.e. nearest neighbors pairs of antiparallel spins, which can be considered as one-particle states. In homogenous systems^{60,86} they have $O(L^{-1})$ momenta, giving rise to a gap of order L^{-2} for FOBC. We expect an analogous scenario for the ground state in the presence of the linear magnetic field $h_x = x/\ell$, that is the ground state is a superposition of one-kink states which switch the chain sites from $|\downarrow\rangle$ to $|\uparrow\rangle$. In particular we argue that this picture describes the crossover region described by the scaling ansatzes (35) and (39), which interpolates between the states with magnetization m_{\pm} , cf. Eq. (7). In this one-kink scenario the local magnetization $m(x)$ and the two-point function $G(0, x)$

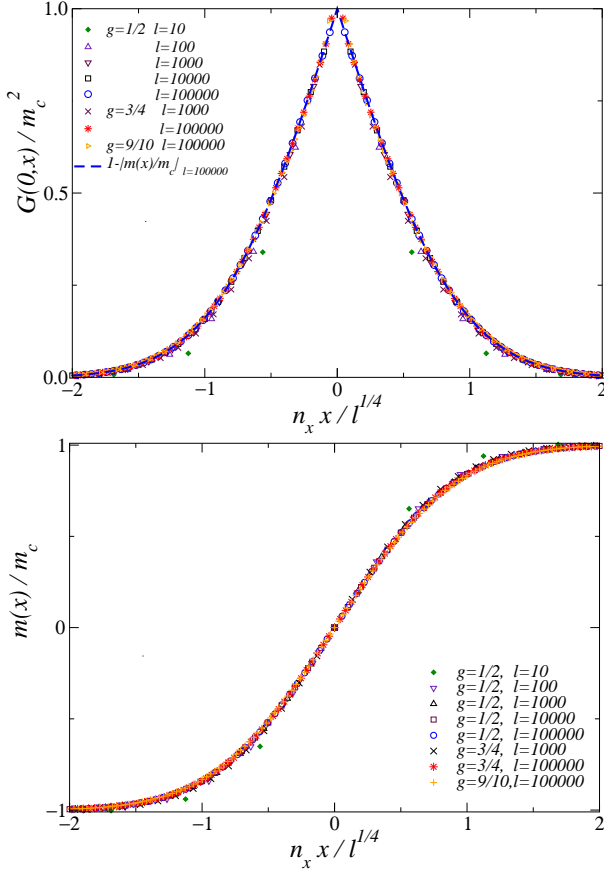


FIG. 7: (Color online) Scaling of the local magnetization $m(x)$ and the two-point function $G(0, x)$, for the Hamiltonian (1) at $g = 1/2, 3/4, 9/10$, with a linear magnetic field, cf. Eq. (3). We plot the ratios $m(x)/m_0$ (bottom) and $G(0, x)/m_c^2$ (top) versus $n_x x / \ell^{1/4}$, where n_x is a normalization, in the figure we use $n_x \approx 1, 3/4, 4/7$ and for $g = 1/2, 3/4, 9/10$ respectively. In the top figure, the comparison with the data of $1 - |m(x)/m_c|$ supports the prediction (45) of the one-kink scenario.

must be asymptotically related. If we define $p(x_1, x_2)$ the probability to find the kink in the interval (x_1, x_2) , then the scaling function f_m is

$$f_m(X) = \frac{m(x)}{m_c} = 2p(-\infty, X) - 1, \quad (42)$$

where $X \equiv x/\ell^\theta$, and m_c is the infinite-volume magnetization, which provides the normalization of the scaling relation (35). Also the value of the two-point function $G(0, x)$ is related to the probability to find the kink in the region $(0, x)$, i.e.

$$f_g(0, X) = \frac{G(0, x)}{m_c^2} = 1 - p(0, X). \quad (43)$$

Since $p(\infty, 0) = 1/2$ by symmetry,

$$p(0, X) = p(-\infty, X) - p(-\infty, 0) = p(-\infty, X) - 1/2 \quad (44)$$

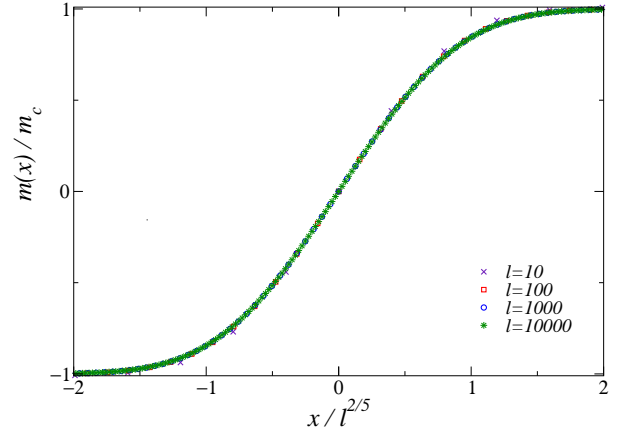


FIG. 8: (Color online) $m(x)/m_c$ versus $x/\ell^{2/5}$, for the Hamiltonian (1) at $g = 1/2$ with a quadratic magnetic field, cf. Eq. (5) with $p = 2$. Like the linear case $p = 1$, the asymptotic one-kink relation (45) is satisfied by the data.

for $X > 0$, and the analog for $X < 0$. Thus we obtain the relation

$$f_g(0, X) = 1 - |f_m(X)|. \quad (45)$$

This relation is confirmed by the data, see the top Fig. 7.

Analogous results are obtained in the case of quadratic dependence, i.e. $p = 2$ in Eq. (5), with $\theta = 2/5$, see Fig. 8. As already mentioned, the scaling behaviors in the $p \rightarrow \infty$ limit must reproduce the FSS of the Ising chain with FOBC.⁶⁰ In particular, for any $g < 1$ and $h = 0$, the FSS functions of the local magnetization and two-point function are given by⁸⁷

$$f_m(X) = X + \frac{1}{\pi} \sin(\pi X), \quad X = x/\ell, \quad (46)$$

$$f_g(X_1, X_2) = 1 - |f_m(X_2) - f_m(X_1)| \quad (47)$$

in the large- ℓ limit keeping X fixed, with $-1 \leq X \leq 1$.

B. Results for the $q = 10$ Potts chain

We now present an analogous analysis of the DMRG data of the $q = 10$ Potts chain with a linearly varying field h_x , cf. Eq. (22). In this case we have that $\theta = 1/3$ according to Eq. (31).

The energy difference of the lowest states is expected to get suppressed as $O(\ell^{-1/3})$, as predicted by Eq. (34) with $\theta = 1/3$ and $z = 1$. This is supported by the analysis of the energy differences $\Delta_\ell = E_1 - E_0$ and $\Delta_{\ell,2} = E_2 - E_0$. As shown in Fig. 9, their data are consistent with an asymptotic behavior

$$\Delta_{\ell,\#} \approx c_1 \ell^{-1/3} + c_2 \ell^{-2/3} + \dots \quad (48)$$

The data of Figs. 10 and 11, for the local magnetization $m(x)$ and the two-point function $G(0, x)$ respectively, appear to approach asymptotic curves when they are plotted versus x/ℓ^θ , supporting the scaling behaviors (35)

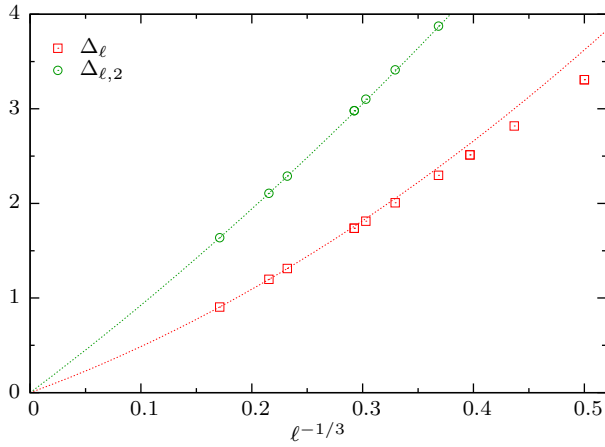


FIG. 9: The ℓ -dependence of the energy differences of the lowest states, i.e. $\Delta_\ell = E_1 - E_0$ and $\Delta_{\ell,2} = E_2 - E_0$. They are consistent with an asymptotic $\ell^{-1/3}$ suppression, as predicted by Eq. (34) with $\theta = 1/3$ and $z = 1$. The dotted lines show fits of the data for the largest chains to the polynomial $c_1 \ell^{-1/3} + c_2 \ell^{-2/3}$.

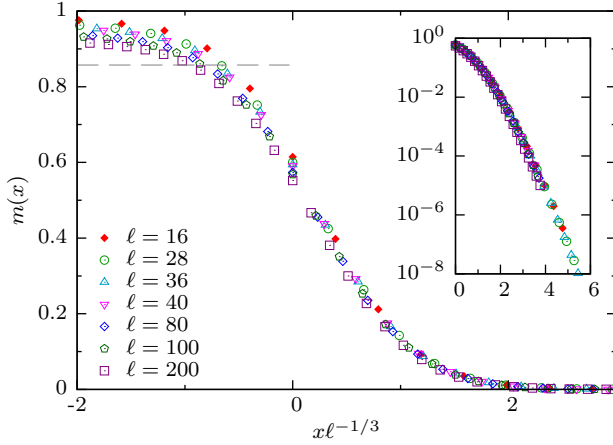


FIG. 10: Scaling of the local magnetisation $m(x)$ of the $q = 10$ Potts chain in the presence of a linear magnetic field h_x . The dashed line shows the expected left asymptotic value m_c , corresponding to $f_m(X) = 1$ for $X \rightarrow -\infty$, cf. Eq. (35). This is slowly approached by the data, due to the expected $O(\ell^{-1/3})$ corrections. The convergence appears much faster for $x > 0$. The inset shows the data for $x > 0$ in logarithmic scale.

and (39). Scaling corrections are also clearly observed, which should get asymptotically suppressed by powers of $\ell^{-\theta}$. Fig. 12 shows the scaling of the energy density, which support the scaling ansatz derived in Sec. III, given by Eqs. (40) and (41).

Let us finally note the similarity of these scaling behaviors with those observed at the first-order classical transition of two-dimensional Potts models in the presence of a gradient temperature along one of the spatial directions, with the other one taken to infinity⁴⁶. Actually, this should not be considered as unexpected, because the quantum Potts chain and the classical two-dimensional

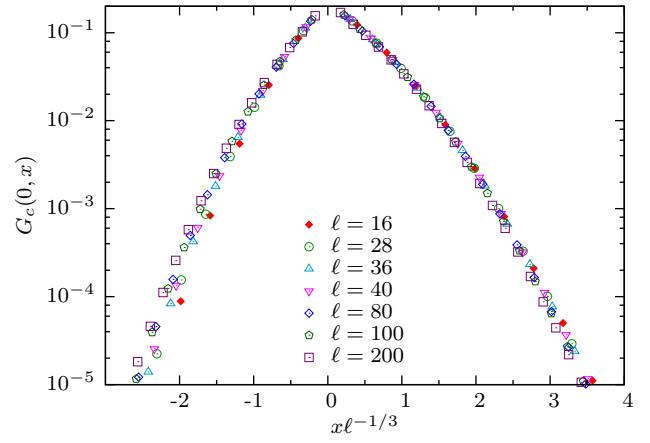


FIG. 11: Scaling of the connected two-point function $G_c(0, x)$, cf. Eq. (38), in the presence of a linear h_x .

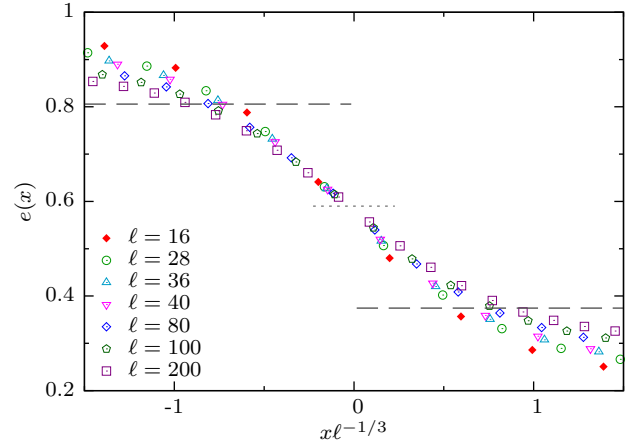


FIG. 12: Scaling of the energy density of the $q = 10$ Potts chain in the presence of a linear h_x . The data appear to approach an asymptotic scaling curve supporting the scaling behavior (40). The dashed lines show the expected asymptotic values e_\pm of the scaling function f_e , cf. Eq. (41). The central dotted line indicates the average value $e_a = (e_+ + e_-)/2$, which seems to be approached by the data at $x = 0$. Scaling corrections are clearly observed, in particular far from the center; they are consistent with the expected (slow) $O(\ell^{-1/3})$ suppression.

Potts model are somehow related by a quantum-to-classical mapping.

V. CONCLUSIONS

We have shown that scaling phenomena emerge at FOQTs in the presence of inhomogeneous conditions, such as those arising from a space-dependent external field, e.g. $h_x \approx x/\ell$ where ℓ is a length scale. In particular, we argue that these scaling phenomena occur in the transition region where the space-dependent parameter $h(x)$ assumes the value h_c corresponding to the FOQT of the

homogenous system.

We put forward scaling ansatzes to describe the behavior at the crossover space region where the system effectively changes its phase, and the typical discontinuities of the FOQT get smoothed out, i.e. when the system is effectively probing the mixed phase. This scaling behavior is characterized by a *critical exponent* θ , cf. Eq. (31), which tells us how the length scale ξ of the observables in the crossover region scales with the length scale ℓ of the inhomogeneous field, i.e. $\xi \sim \ell^\theta$. The exponent θ depends on some general features of the external field giving rise to the inhomogeneity, such as the effective power law of the space dependence at the transition point and the way it is coupled to the system variables. This scaling behavior is such that the typical singularities of FOQT must be recovered in the limit $\ell \rightarrow \infty$ where the system tend to become homogenous. Generally $\theta < 1$, approaching one in the limit of an infinite power law, i.e. $p \rightarrow \infty$ in Eq. (5), where the inhomogeneous scaling behavior must match the FSS behavior of homogenous systems with appropriate boundary conditions^{60,61}.

We provide numerical evidence of such scaling phenomena for two classes of FOQTs. We consider the FOQT of quantum Ising chains, which are driven by a parallel

magnetic field when the system is in the ferromagnetic phase, and those of the q -state Potts chain for $q > 4$ which is driven by an even temperature-like parameter with a discontinuity in the ground-state energy density.

Our approach is quite general: the results can be straightforwardly extended to other systems undergoing FOQTs and other sources of inhomogeneities smoothing out the singularities of the transition.

These peculiar inhomogeneous scaling phenomena should be observable in experiments of physical systems, requiring essentially the possibility of measuring local quantities and controlling/tuning the length-scale of the inhomogeneity. Such conditions may be realized in cold-atom experiments, in particular in optical lattices, when the atomic system is such to have a FOQT in homogenous conditions, but the space dependence of the effective chemical potential (arising from the trap) smooths out its discontinuities. Around this region we should observe a crossover region with the scaling features put forward in this paper. For example, FOQT lines are expected in the zero-temperature phase diagrams of atomic systems described by multicomponents Bose-Hubbard models⁴, with spin-orbit coupling and synthetic gauge fields, see, e.g., Refs. 54–58.

-
- ¹ L.D. Landau and E.M. Lifshitz, *Statistical Physics* (Pergamon Press, 1969).
 - ² K.G. Wilson, in *Nobel Lectures in Physics 1981-1990*, G. Ekspong Ed., World Scientific Publ., Singapore, 1993; K.G. Wilson and J. Kogut, Phys. Rep. **12**, 77 (1974).
 - ³ S. Sachdev, *Quantum Phase Transitions*, (Cambridge University Press, 2011, 2nd ed.)
 - ⁴ I. Bloch, J. Dalibard, and W. Zwerger, Rev. Mod. Phys. **80**, 885 (2008).
 - ⁵ M. R. Moldover, J. V. Sengers, R. W. Gammon, and R. J. Hocken, Rev. Mod. Phys. **51**, 79 (1979).
 - ⁶ K. Damle, T. Senthil, S.N. Majumdar, and S. Sachdev, Europhys. Lett. **36**, 7 (1996).
 - ⁷ S. Wessel, F. Alet, M. Troyer, and G.G. Batrouni, Phys. Rev. A **70**, 053615 (2004).
 - ⁸ M. Rigol and A. Muramatsu, Phys. Rev. A **70**, 031603 (2004); Phys. Rev. A **72**, 013604 (2005).
 - ⁹ S. Fölling, A. Widera, T. Müller, F. Gerbier, and I. Bloch, Phys. Rev. Lett. **97**, 060403 (2006).
 - ¹⁰ Q. Niu, I. Carusotto, and A.B. Kuklov, Phys. Rev. A **73**, 053604 (2006).
 - ¹¹ D. Belitz, T.R. Kirkpatrick, and R. Saha, Phys. Rev. Lett. **99**, 147203 (2007).
 - ¹² T. Platini, D. Karevski, and L. Turban, J. Phys A **40**, 1467 (2007).
 - ¹³ R.B. Diener, Q. Zhou, H. Zhai, and T.L. Ho, Phys. Rev. Lett. **98**, 180404 (2007).
 - ¹⁴ T. Donner, S. Ritter, T. Bourdel, A. Öttl, M. Köhl, and T. Esslinger, Science **315**, 1556 (2007).
 - ¹⁵ M. Holzmann and W. Krauth, Phys. Rev. Lett. **100**, 190402 (2008).
 - ¹⁶ N. Gemelke, X. Zhang, C.-L. Hung, and C. Chin, Nature **460**, 995 (2009).
 - ¹⁷ A. Bezett and P.B. Blakie, Phys. Rev. A **79**, 033611 (2009).
 - ¹⁸ E. Taylor, Phys. Rev. A **80**, 023612 (2009).
 - ¹⁹ M. Campostrini and E. Vicari, Phys. Rev. Lett. **102**, 240601 (2009); (E) **103**, 269901 (2009).
 - ²⁰ R.N. Bisset, M.J. Davis, T.P. Simula, and P.B. Blakie, Phys. Rev. A **79**, 033626 (2009).
 - ²¹ Q. Zhou, Y. Kato, N. Kawashima, and N. Trivedi, Phys. Rev. Lett. **103**, 085701 (2009).
 - ²² M. Rigol, G.G. Batrouni, V.G. Rousseau, and R.T. Scalettar, Phys. Rev. A **79**, 053605 (2009).
 - ²³ I. Hen and M. Rigol, Phys. Rev. A **82**, 043634 (2010).
 - ²⁴ S. Trotzky, L. Pollet, F. Gerbier, U. Schnorrberger, I. Bloch, N.V. Prokofev, B. Svistunov, and M. Troyer, Nat. Phys. **6**, 998 (2010).
 - ²⁵ M. Campostrini and E. Vicari, Phys. Rev. A **81**, 023606 (2010).
 - ²⁶ Q. Zhou and T.-L. Ho, Phys. Rev. Lett. **105**, 245702 (2010).
 - ²⁷ T.-L. Ho and Q. Zhou, Nat. Phys. **6**, 131 (2010).
 - ²⁸ L. Pollet, N.V. Prokofev, and B.V. Svistunov, Phys. Rev. Lett. **104**, 245705 (2010).
 - ²⁹ L. Pollet, N.V. Prokofev, and B.V. Svistunov, Phys. Rev. Lett. **105**, 199601 (2010).
 - ³⁰ S. Nascimbene, N. Nayon, F. Chevy, and C. Salomon, New J. Phys. **12**, 103026 (2010).
 - ³¹ Q. Zhou, Y. Kato, N. Kawashima, and N. Trivedi, Phys. Rev. Lett. **105**, 199602 (2010).
 - ³² M. Campostrini and E. Vicari, Phys. Rev. A **81**, 063614 (2010); Phys. Rev. A **82**, 063636 (2010); J. Stat. Mech. (2010) P08020; E04001 (2010).
 - ³³ S.L.A. de Queiroz, R.R. dos Santos, and R.B. Stinchcombe, Phys. Rev. E **81**, 051122 (2010).
 - ³⁴ S. Fang, C.-M. Chung, P.-N. Ma, P. Chen, and D.-W. Wang, Phys. Rev. A **83**, 031605(R) (2011).

- ³⁵ X. Zhang, C.-L. Hung, S.-K. Tung, N. Gemelke, and C. Chin, *New J. Phys.* **13**, 045011 (2011).
- ³⁶ F. Crecchi and E. Vicari, *Phys. Rev. A* **83**, 035602 (2011).
- ³⁷ K.W. Mahmud, E.N. Duchon, Y. Kato, N. Kawashima, R.T. Scalettar, and N. Trivedi, *Phys. Rev. B* **84**, 054302 (2011).
- ³⁸ K.R.A. Hazzard and E.J. Mueller, *Phys. Rev. A* **84**, 013604 (2011).
- ³⁹ G. Ceccarelli, C. Torrero, and E. Vicari, *Phys. Rev. A* **85**, 023616 (2012); *Phys. Rev. B* **87**, 024513 (2013).
- ⁴⁰ L. Pollet, *Rep. Prog. Phys.* **75**, 094501 (2012).
- ⁴¹ G. Ceccarelli and C. Torrero, *Phys. Rev. A* **85**, 053637 (2012).
- ⁴² Y. Khorramzadeh, Fei Lin, and V.W. Scarola, *Phys. Rev. A* **85**, 043610 (2012).
- ⁴³ J. Carrasquilla and M. Rigol, *Phys. Rev. A* **86**, 043629 (2012).
- ⁴⁴ G. Ceccarelli, J. Nespolo, A. Pelissetto, and E. Vicari, *Phys. Rev. B* **88**, 024517 (2013).
- ⁴⁵ G. Ceccarelli and J. Nespolo, *Phys. Rev. B* **89**, 054504 (2014).
- ⁴⁶ C. Bonati, M. D'Elia, and E. Vicari, *Phys. Rev. E* **89**, 062132 (2014).
- ⁴⁷ M.E. Fisher, M.N. Barber, and D. Jasnow, *Phys. Rev. A* **8**, 1111 (1973).
- ⁴⁸ J. Cardy, *Finite-Size Scaling*, North Holland, Amsterdam, 1988.
- ⁴⁹ V. Piazza, V. Pellegrini, F. Beltram, W. Wegscheider, T. Jungwirth, and A.H. MacDonald, *Nature* **402**, 638 (1999).
- ⁵⁰ T. Vojta, D. Belitz, T.R. Kirkpatrick, and R. Narayanan, *Ann. Phys. (Leipzig)* **8**, 593 (1999).
- ⁵¹ M. Uhlarz, C. Pfleiderer, and S.M. Hayden, *Phys. Rev. Lett.* **93**, 256404 (2004).
- ⁵² C. Pfleiderer, *J. Phys.: Cond. Matter* **17**, S987 (2005).
- ⁵³ W. Knafo, S. Raymond, P. Lejay, and J. Flouquet, *Nature Phys.* **5**, 753 (2009).
- ⁵⁴ E. Jechelmann, *Phys. Rev. Lett.* **89**, 236401 (2002).
- ⁵⁵ G.G. Batrouni, V.G. Rousseau, and R.T. Scalettar, *Phys. Rev. Lett.* **102**, 140402 (2009).
- ⁵⁶ J. Radic, A. Di Ciolo, K. Sun, and V. Galitski, *Phys. Rev. Lett.* **109**, 085303 (2012).
- ⁵⁷ S. Peotta, L. Mazza, E. Vicari, M. Polini, R. Fazio, and D. Rossini, *J. Stat. Mech.* (2014) P09005.
- ⁵⁸ M. Piraud, Z. Cai, I.P. McCulloch, and U. Schollwöck, *Phys. Rev. A* **89**, 063618 (2014).
- ⁵⁹ U. Schollwöck, *Rev. Mod. Phys.* **77**, 259 (2005).
- ⁶⁰ M. Campostrini, J. Nespolo, A. Pelissetto, and E. Vicari, *Phys. Rev. Lett.* **113**, 070402 (2014).
- ⁶¹ M. Campostrini, J. Nespolo, A. Pelissetto, and E. Vicari, arXiv:1410.8662.
- ⁶² P. Pfeuty, *Ann. Phys.* **57**, 79 (1970).
- ⁶³ S. Giorgini, L.P. Pitaevskii, and S. Stringari, *Rev. Mod. Phys.* **80**, 1215 (2008).
- ⁶⁴ T. Esslinger, *Ann. Rev. Cond. Mat. Phys.* **1**, 129 (2010).
- ⁶⁵ X.-W. Guan, M.T. Batchelor, and C. Lee, *Rev. Mod. Phys.* **85**, 1633 (2013).
- ⁶⁶ A. Angelone, M. Campostrini, and E. Vicari, *Phys. Rev. A* **89**, 023635 (2014).
- ⁶⁷ R.B. Potts, *Math. Proc. Camb. Phil. Soc.* **48**, 106 (1952).
- ⁶⁸ F.Y. Wu, *Rev. Mod. Phys.* **54**, 235 (1982).
- ⁶⁹ R.J. Baxter, *J. Phys. C: Solid State Phys.* **6**, L445 (1973); R.J. Baxter, H.N.V. Temperley, and S.E. Ashley, *Proc. R. Soc. Lond. A* **538**, 535 (1978).
- ⁷⁰ J. Sólyom and P. Pfeuty, *Phys. Rev. B* **24**, 218 (1981).
- ⁷¹ F. Iglói and J. Sólyom, *J. Phys. C: Solid State Phys.* **16**, 2833 (1983).
- ⁷² B. Nienhuis and M. Nauenberg, *Phys. Rev. Lett.* **35**, 477 (1975).
- ⁷³ M.E. Fisher and A.N. Berker, *Phys. Rev. B* **26**, 2507 (1982);
- ⁷⁴ V. Privman and M. E. Fisher, *J. Stat. Phys.* **33**, 385 (1983).
- ⁷⁵ M. E. Fisher and V. Privman, *Phys. Rev. B* **32**, 447 (1985).
- ⁷⁶ M.S.S. Challa, D.P. Landau, and K. Binder, *Phys. Rev. B* **34**, 1841 (1986).
- ⁷⁷ V. Privman ed., *Finite Size Scaling and Numerical Simulation of Statistical Systems* (World Scientific, Singapore, 1990).
- ⁷⁸ J. Lee and J.M. Kosterlitz, *Phys. Rev. B* **43**, 3265 (1991).
- ⁷⁹ C. Borgs and R. Kotecký, *Phys. Rev. Lett.* **68**, 1734 (1992).
- ⁸⁰ A. Billoire, T. Neuhaus, and B.A. Berg, *Nucl. Phys. B* **396**, 779 (1993).
- ⁸¹ K. Vollmayr, J.D. Reger, M. Scheucher, and K. Binder, *Z. Phys. B* **91**, 113 (1993).
- ⁸² F. Iglói and E. Carlon, *Phys. Rev. B* **59**, 3783 (1999).
- ⁸³ P. Calabrese, P. Parruccini, A. Pelissetto, and E. Vicari, *Phys. Rev. B* **70**, 174439 (2004).
- ⁸⁴ S.L. Sondhi, S.M. Girvin, J.P. Carini, and D. Shahar, *Rev. Mod. Phys.* **69**, 315 (1997).
- ⁸⁵ M. Campostrini, A. Pelissetto and E. Vicari, *Phys. Rev. B* **89**, 094516 (2014).
- ⁸⁶ G.G. Cabrera and R. Jullien, *Phys. Rev. B* **35**, 7062 (1987).
- ⁸⁷ M. Campostrini, A. Pelissetto, and E. Vicari, in preparation.